

Optical properties of mist CVD grown α -Ga₂O₃

Usman UI Muazzam¹, Prasad chavan¹, Srinivasan Raghavan¹, R. Muralidharan¹, Digbijoy N Nath¹

¹ Centre for Nano Science and Engineering, Indian Institute of Science, 560012, Bangalore, India

We report on the study of optical properties of mist CVD grown α -Ga₂O₃ with the observation of excitonic absorption in spectral responsivity measurements. 163 nm of Ga₂O₃ was grown on sapphire using Ga-(acac)₃ as the starting solution at a substrate temperature of 450°C. The film was found to be crystalline and of α -phase with an on-axis full width at half maximum (FWHM) of 92 arcsec as confirmed from X-ray diffraction scans. The Tauc's plot extracted from absorption spectroscopy exhibited two transitions in the UV regime at 5.3 eV and 5.6 eV, corresponding to excitonic absorption and direct band-to-band transition respectively. The binding energy of exciton was extracted to be 114 meV from spectral responsivity (S.R) measurements. Further, metal-semiconductor-metal (MSM) photodetectors (PD) with lateral inter-digitated geometry were fabricated on the film. A sharp band edge was observed at 230 nm (~ 5.6 eV) in the spectral response with peak responsivity of ~1 A/W at a bias of 20 V. The UV to visible rejection ratio was found to be ~ 100 while the dark current was measured to be ~ 0.1 nA.

The various polymorphs of Ga₂O₃, with their wide band gap of 4.6-5.3 eV^{1,2}, have attracted attention of the device community for their promises in the areas of high-power switching³, deep-UV optoelectronics⁴, gas sensors⁵, high-temperature and transparent electronics⁶. UV-C photodetectors for instance, are useful in UV astronomy, bio-medical and forensic applications, and for missile plume detection in the strategic sector⁷⁻⁹. Although the β phase is the most stable among the five different polymorphs (α , β , γ , ϵ , δ) of Ga₂O₃ and thus has been the most widely investigated, there has been an increasing interest in α -Ga₂O₃ in recent times. It has a corundum crystal structure and has been predicted to have the highest bandgap (~ 5.3 eV¹⁰) among all the polymorphs of Ga₂O₃. This makes α -Ga₂O₃ an attractive candidate for ultra-high breakdown transistors and deep-UV opto-electronics at sub-240 nm wavelengths. The growth of α -Ga₂O₃, which requires relatively low temperatures (430°C – 470°C)¹⁰, has been reported using approaches such as atomic layer deposition (ALD), mist chemical vapor deposition and molecular beam epitaxy^{11,12}. Although there is a report on the demonstration of field effect transistor (FET) based on mist CVD grown α -Ga₂O₃¹³, the investigation of the growth as well as structural, optical and electrical transport properties of this emerging polymorph of Ga₂O₃ is still at an embryonic stage. In this letter, we report on the study of optical – in particular excitonic - properties of mist CVD grown α -Ga₂O₃ with a subsequent realization of a high-responsivity solar blind UV-C photodetectors.

The mist CVD system used for the growths has been developed in-house and consists of two parts, the reactor and the mist generator. A volume of 0.33 mole 5N pure gallium acetylacetonate Ga(acac)₃ dissolved in de-ionised water (DI) was used as the source of gallium precursor. Small amount (0.1 ml) of HCl was added to ensure the complete dissolution of Ga(acac)₃ in DI water. This solution was then ultra-sonicated at a frequency of 1.6 MHz using the mist-generator. The generated mist was directed to the deposition zone using N₂ (500 sccm) as carrier gas. c-plane sapphire wafer of 2-inch diameter was diced into 1 cm x 1 cm pieces and were solvent cleaned in acetone, isopropyl alcohol and rinsed with DI water. For each growth run, a piece of sapphire was placed inside the deposition zone using a quartz tube with diameter of 40 mm. The growth was carried out for one hour at a temperature of 450 °C and at atmospheric pressure.

The XRD scans were carried out using a Rigaku SmartLab, Cu-K α radiation X-ray diffraction system. The film grown on sapphire was confirmed to be α -Ga₂O₃ from θ -2 θ scan. Figure 1 shows (0006) reflection of α -Ga₂O₃, and the inset to figure 1 shows the symmetric rocking curve with an FWHM of 92.2 arcsec indicative of a low screw dislocation density in the epi-layer. The surface morphology of the as-deposited film was studied using atomic force microscope (Dimension ICON, Bruker) and the rms roughness was found to be 2 nm as shown in Figure 2(a), which confirms the smoothness of the film. The film thickness was found to be 163 nm from ellipsometry measurements. Figure 2(b) shows the image of the as-grown film as obtained from scanning electron microscope (GEMINI Ultra 55, FE-SEM, Carl Zeiss), indicating that the layer is continuous and uniform.

a) Corresponding author email: usmaanm@iisc.ac.in
digbijoy@iisc.ac.in

Absorption measurement was done using UV-Vis setup (UV-3600, UV-VIS-NIR spectrophotometer, Shimadzu). The Tauc's plot (figure 3) exhibited a distinct kink in addition to the primary absorption edge. The first edge at 5.3 eV corresponds to excitonic transition while the kink with sharp transition corresponds to band-to-band absorption at 5.6 eV when extrapolated linearly to intersect the x-axis and indicates the band gap of α -Ga₂O₃.

Photodetectors with metal semiconductor metal (MSM) layout in an interdigitated geometry were fabricated on the as-grown α -Ga₂O₃ sample using standard i-line lithography process. The device schematic is shown in Fig. 4(a). Ni (20nm)/Au (100nm) stack was deposited using sputtering to form Schottky contact. Each MSM detector as shown in Fig. 4(b), comprised of seventeen pairs of interdigitated fingers where each finger had a width of 4 μ m and the finger spacing was 6 μ m. The active area of each device was 260 μ m x 300 μ m.

Spectral responsivity (SR) measurement was done using a quantum efficiency setup, the details of which are reported elsewhere¹⁴. The SR spectra exhibited a primary peak at 230 nm corresponding to band-to-band absorption while an excitonic peak could be observed at 235 nm. The binding energy of exciton, estimated from the difference between the two peaks, was found to be 114 meV, which is in close agreement with earlier reported values¹⁵. This is also the first report of observation of excitonic peak in spectral response of any polymorph of gallium oxide.

Raman spectra was recorded in the backscattering geometry using 532 nm laser, the light was then collected using 100x objective in backscattered geometry and analysed using LabRAM HR, Horiba spectrometer. Figure 5. shows Raman spectra of α -Ga₂O₃. The corundum structure of α -Ga₂O₃ belongs to -3m (D_{3d}) point group and R-3c (D_{3d}⁶) space group. According to group theory analysis the irreducible representation of zone-centre optical mode is:

$$\Gamma = 2A_{1g} + 2A_{1u} + 3A_{2g} + 2A_{2u} + 5E_g + 4E_u \quad (1)$$

In addition, unit cell of α -Ga₂O₃ is centrosymmetric thus all vibrations that are Raman allowed are infrared forbidden and vice-versa. The A_{1g} and E_g are Raman active, A_{2u} and E_u are infrared active, and A_{1u} and A_{2g} vibrations are neither Raman nor infrared active. The spectrum shows A_{1g}(LO) phonon mode at 216 cm⁻¹. This mode is attributed to Ga atoms vibrating against each other along c-axis. The high frequency E_g mode at 430 cm⁻¹ is due to lighter O atom vibrations perpendicular to c-axis¹⁶. Low intensity of Raman modes of α -Ga₂O₃ may be due to thinner sample.

In most of the oxide semiconductors, the excitonic binding energy is larger than the Rydberg exciton effective energy which is given by:

$$E_{\text{exo}} = R_y \frac{\mu}{\left(\frac{\epsilon_s}{\epsilon_0}\right)^2} \quad (2)$$

$$\frac{1}{\mu} = \frac{1}{m_e} + \frac{1}{m_h}$$

Here, R_y is the Rydberg energy which has value of 13.6 eV, μ is the reduced mass of exciton, m_o is free electron mass, ϵ_s the static dielectric constant of Ga₂O₃ which is 10¹⁷. Since m_h >> m_e, μ is approximately taken as m_e which is 0.276m_o¹⁸. From equation (1), the excitonic binding energy is found to be around 37.53 meV which is underestimated because we have not considered the interaction between LO phonons and excitons. Polar materials have more than one atom per unit cell having non-zero Born effective charge; thus, atomic displacement corresponding to polar LO phonons can give rise to microscopic Born effective electric fields at long wavelengths leading to strong coupling between LO phonons and excitons¹⁹. Interaction between polar optical phonons and excitons can be described using Frohlich coupling constant, which is given by²⁰:

$$\alpha_F = \frac{q^2}{8\pi\epsilon_0\hbar} \sqrt{\frac{2m_c}{\hbar\omega_0}} \left(\frac{1}{\epsilon_\infty} - \frac{1}{\epsilon_s}\right) \quad (3)$$

Using equations (2) and (3) E_{ex} can be estimated to be 91.71meV.

This value is very close to the value estimated from spectral responsivity. To estimate the dissociation field for exciton, polaron (coupling of LO phonon with electron) radius was calculated using²¹:

$$a_p = \sqrt{\frac{2\hbar}{m\omega_{LO}}} \quad (4)$$

where a_p is Polaron radius. From equation (4), a_p was found to be 32.2 Å, which corresponded to a dissociation field of 0.354 MV/cm.

Figure 6(a) shows the variation of responsivity with wavelength at different voltages on linear scale (5 V, 10 V, 15 and 20 V). Inset to figure 6(a) shows the same in log scale. The peak responsivity was measured to be 0.95 A/W at 230 nm at a bias of 20 V. The UV to visible rejection ratio was calculated by dividing the responsivity value at 230 nm by that at 400 nm, and was found to be $> 10^2$ at 20 V.

Figure 6(b) shows the current-voltage (I-V) characteristic of the detectors under dark and under illumination at 230 nm. The photo current was found to be 85 nA while the dark current was measured to be 137 pA at an applied bias of 20 V, indicating a photo-to-dark current ratio exceeding two orders of magnitude.

Figure 6(c) shows the variation of peak responsivity with applied voltage at an illumination of 230 nm. The peak responsivity was found to increase with an increase in applied voltage.

The theoretical value of responsivity at 230 nm, assuming a quantum efficiency of 100%, is 185 mA/W. This is much smaller than the peak responsivity value of 518 mA/W at 5 V (at 230 nm) measured in this work, even at a relatively low bias of 5 V, implying that there is gain in the devices²²⁻²⁴. This gain could be because of oxygen vacancies²⁵, which act as hole trapping centres in the bulk of the semiconductor which could lead to photoinduced barrier lowering²² resulting in an increase in transit time.

In conclusion, we have reported on the study of growth and photo-response properties of mist CVD grown α -Ga₂O₃ on c-plane sapphire. Solar blind deep-UV photodetectors realized on these samples exhibited high responsivity of 0.5 A/W at 5 V bias with a sharp peak at 5.5 eV, low dark current of ~ pA and UV-to-visible rejection ratio exceeding two orders of magnitude. We reported the first observation of excitonic peak in spectral responsivity with an excitonic binding energy of 114 meV. This work is expected to aid further in the understanding of optical properties of α -Ga₂O₃ Towards realizing high-performance deep-UV optoelectronics based on gallium oxide.

This work was supported in part by the Ministry of Electronics and Information Technology (MeitY), and in part by the DST through the NNetRA.

References

- ¹ T. Wang, W. Li, C. Ni, and A. Janotti, *Phys. Rev. Appl.* **10**, 1 (2018).
- ² Y. Chen, X. Xia, H. Liang, Q. Abbas, Y. Liu, and G. Du, *Cryst. Growth Des.* **18**, 1147 (2018).
- ³ M. Higashiwaki, K. Sasaki, H. Murakami, Y. Kumagai, A. Koukitu, A. Kuramata, T. Masui, and S. Yamakoshi, *Semicond. Sci. Technol.* **31**, 34001 (2016).
- ⁴ A. Singh Pratiyush, S. Krishnamoorthy, S. Vishnu Solanke, Z. Xia, R. Muralidharan, S. Rajan, and D.N. Nath, *Appl. Phys. Lett.* **110**, 1 (2017).
- ⁵ A. Trinchì, W. Włodarski, and Y.X. Li, *Sensors Actuators, B Chem.* **100**, 94 (2004).
- ⁶ M. Orita, H. Ohta, M. Hirano, and H. Hosono, *Appl. Phys. Lett.* **77**, 4166 (2000).
- ⁷ L. Sang, M. Liao, and M. Sumiya, *Sensors (Switzerland)* **13**, 10482 (2013).
- ⁸ E. Monroy, F. Omnès, and F. Calle, *Semicond. Sci. Technol.* **18**, (2003).
- ⁹ M. Razeghi, *Proc. IEEE* **90**, 1006 (2002).
- ¹⁰ D. Shinohara and S. Fujita, *Jpn. J. Appl. Phys.* **47**, 7311 (2008).
- ¹¹ S.H. Lee, K.M. Lee, Y.-B. Kim, Y.-J. Moon, S. Bin Kim, D. Bae, T.J. Kim, Y.D. Kim, S.-K. Kim, and S.W. Lee, *J. Alloys Compd.* **780**, 400 (2018).
- ¹² X. Chen, Y. Xu, D. Zhou, S. Yang, F.F. Ren, H. Lu, K. Tang, S. Gu, R. Zhang, Y. Zheng, and J. Ye, *ACS Appl. Mater. Interfaces* **9**, 36997 (2017).
- ¹³ G.T. Dang, T. Kawaharamura, M. Furuta, and M.W. Allen, *IEEE Trans. Electron Devices* **62**, 3640 (2015).
- ¹⁴ P. Jaiswal, U. Ul Muazzam, A.S. Pratiyush, N. Mohan, S. Raghavan, R. Muralidharan, S.A. Shivashankar, and D.N. Nath, *Appl. Phys. Lett.* **112**, (2018).

- ¹⁵ A. Segura, L. Artús, R. Cuscó, R. Goldhahn, and M. Feneberg, *Phys. Rev. Mater.* **1**, 024604 (2017).
- ¹⁶ R. Cuscó, N. Domènech-Amador, T. Hatakeyama, T. Yamaguchi, T. Honda, and L. Artús, *J. Appl. Phys.* **117**, (2015).
- ¹⁷ M. Higashiwaki, K. Sasaki, A. Kuramata, T. Masui, and S. Yamakoshi, *Phys. Status Solidi Appl. Mater. Sci.* **211**, 21 (2014).
- ¹⁸ H. He, R. Orlando, M.A. Blanco, R. Pandey, E. Amzallag, I. Baraille, and M. Rérat, *Phys. Rev. B - Condens. Matter Mater. Phys.* **74**, 1 (2006).
- ¹⁹ Peter Y. Yu and M. Cardona, *Fundamentals of Semiconductors Physics and Materials Properties*, Fourth Edi (Springer, 2010).
- ²⁰ N. Tanen, H. (Grace) Xing, Z. Guo, A. Verma, D. Jena, N. Ma, and T. Luo, *Appl. Phys. Lett.* **109**, 212101 (2016).
- ²¹ J.T. Devreese, ArXiv:1012.4576 [Cond-Mat.Other] (2015).
- ²² O. Katz, V. Garber, B. Meyler, G. Bahir, and J. Salzman, *Appl. Phys. Lett.* **79**, 1417 (2001).
- ²³ H. Srour, J.P. Salvestrini, A. Ahaitouf, S. Gautier, T. Moudakir, B. Assouar, M. Abarkan, S. Hamady, and A. Ougazzaden, *Appl. Phys. Lett.* **99**, 3 (2011).
- ²⁴ F. Xie, H. Lu, X. Xiu, D. Chen, P. Han, R. Zhang, and Y. Zheng, *Solid. State. Electron.* **57**, 39 (2011).
- ²⁵ A.M. Armstrong, M.H. Crawford, A. Jayawardena, A. Ahyi, and S. Dhar, *J. Appl. Phys.* **119**, 1 (2016).

Figures

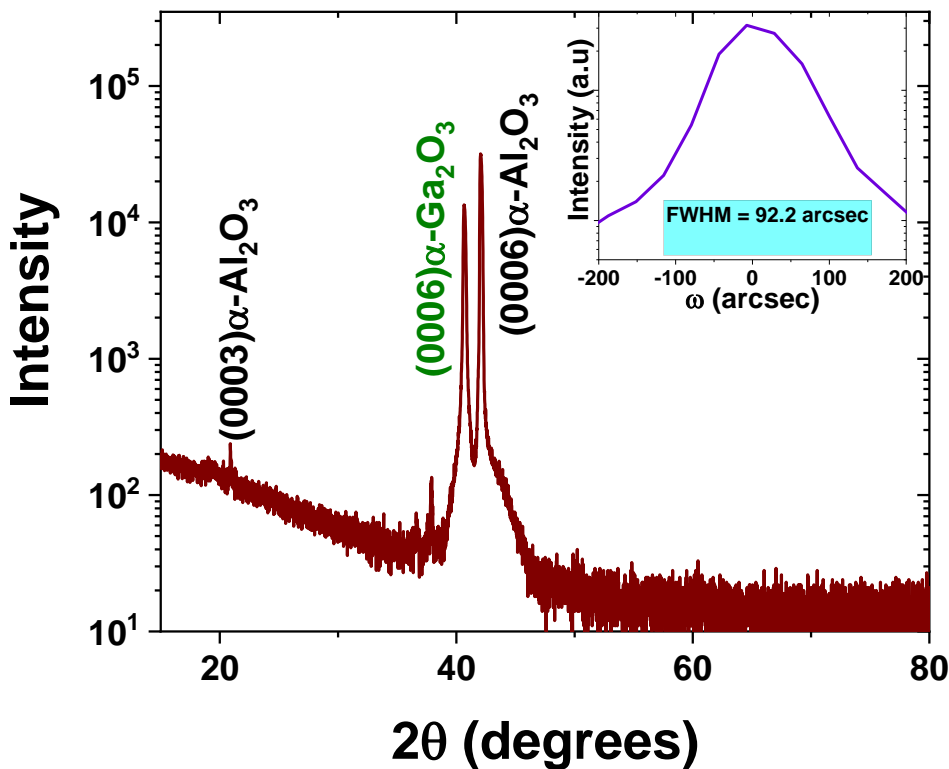


Figure: 1. XRD θ - 2θ diffraction pattern of as deposited film of α - Ga_2O_3 , inset shows rocking curve plot of (0006) peak of α - Ga_2O_3 with FWHM of 92.2 arcsec.

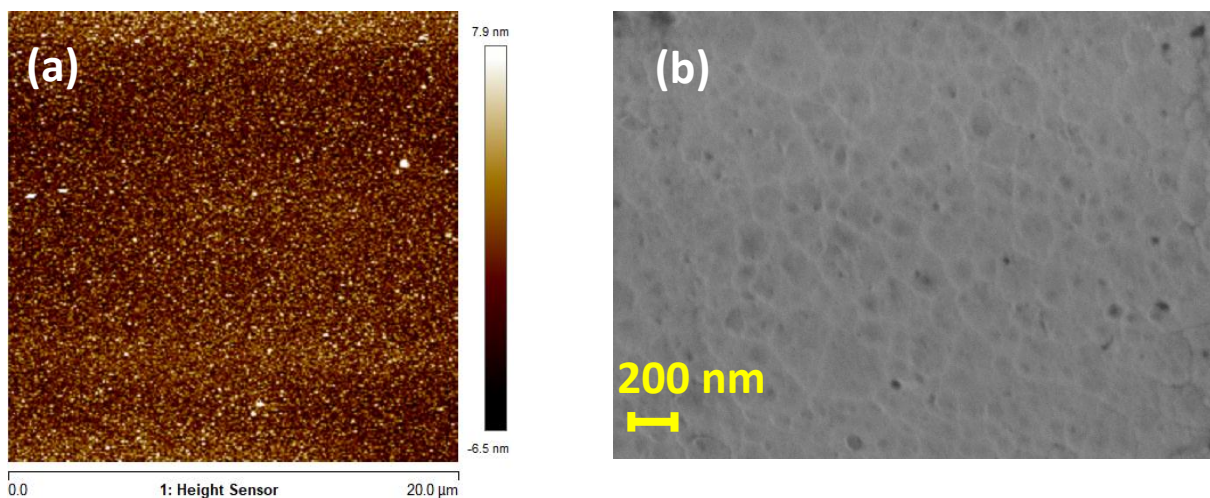


Figure2. (a)AFM scan image showing R.M.S roughness of 2 nm. (b) SEM micrograph showing smooth morphology of as deposited film.

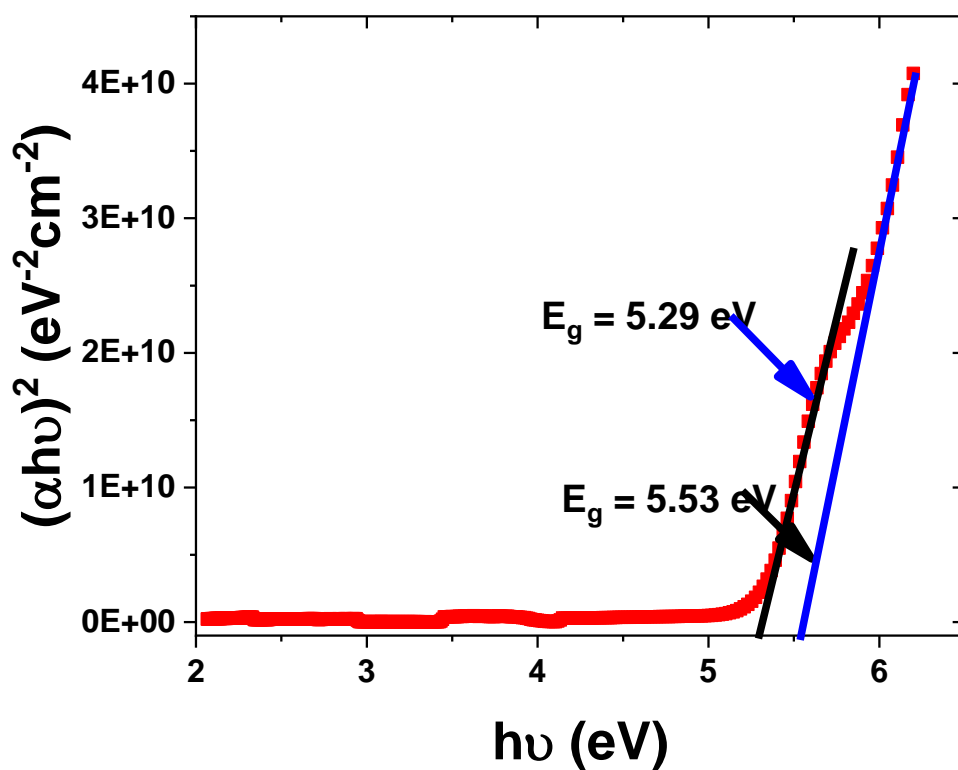


Figure3. Tauc's plot showing two transitions.

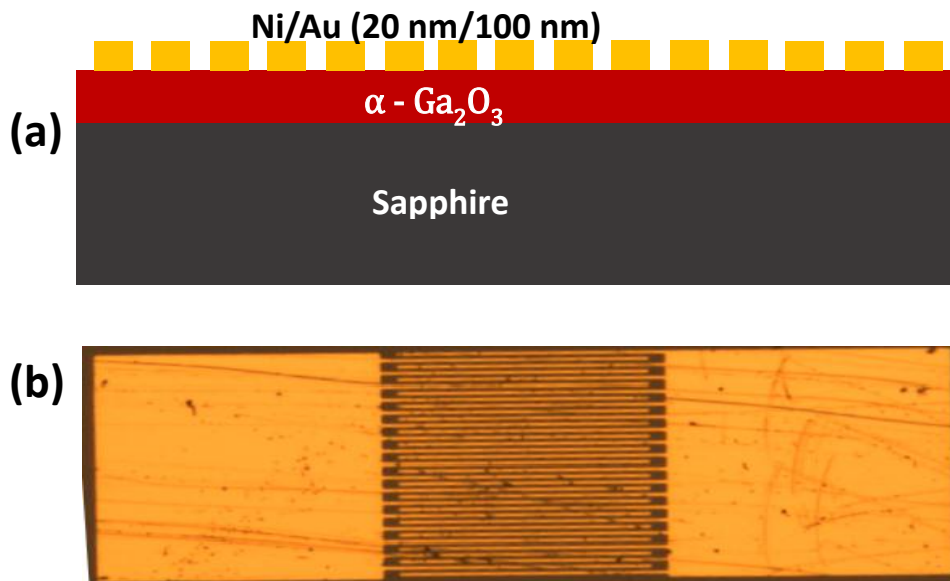


Figure4 (a) Schematic of MSM photodetector (side view). (b) Optical micrograph of MSM photodetector (top view).

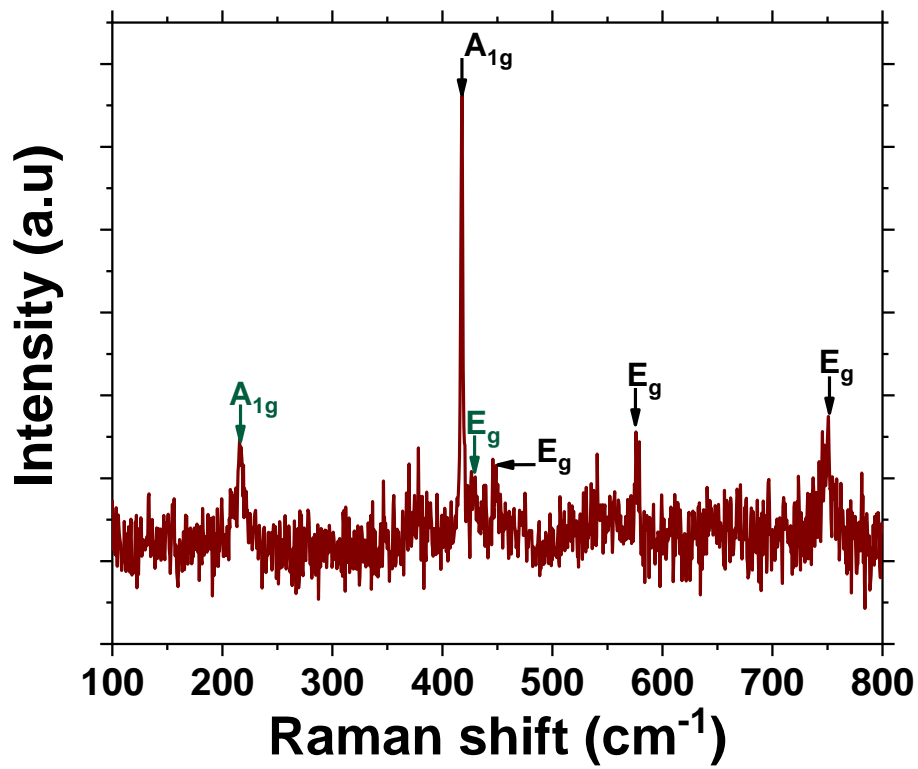


Figure5 (a). Raman spectra of as deposited film. The green and black labels correspond to α -Ga₂O₃ and Sapphire peaks respectively.

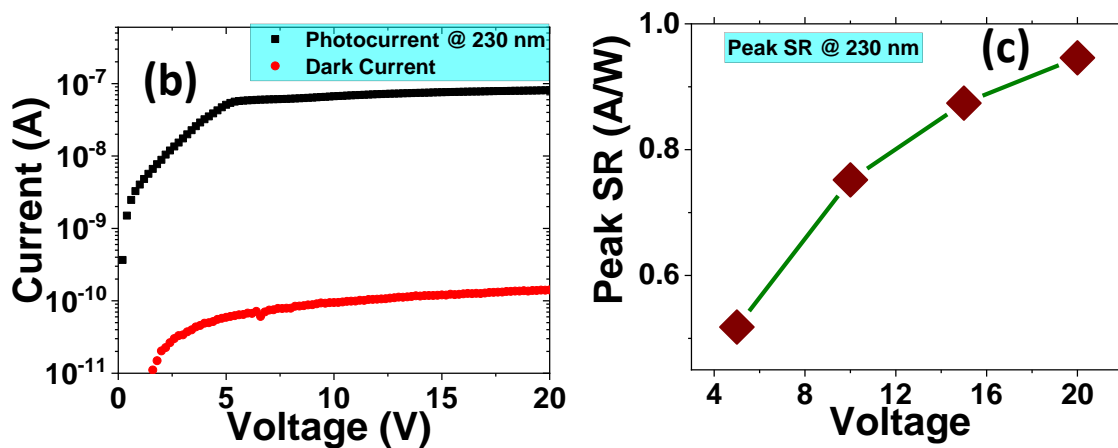
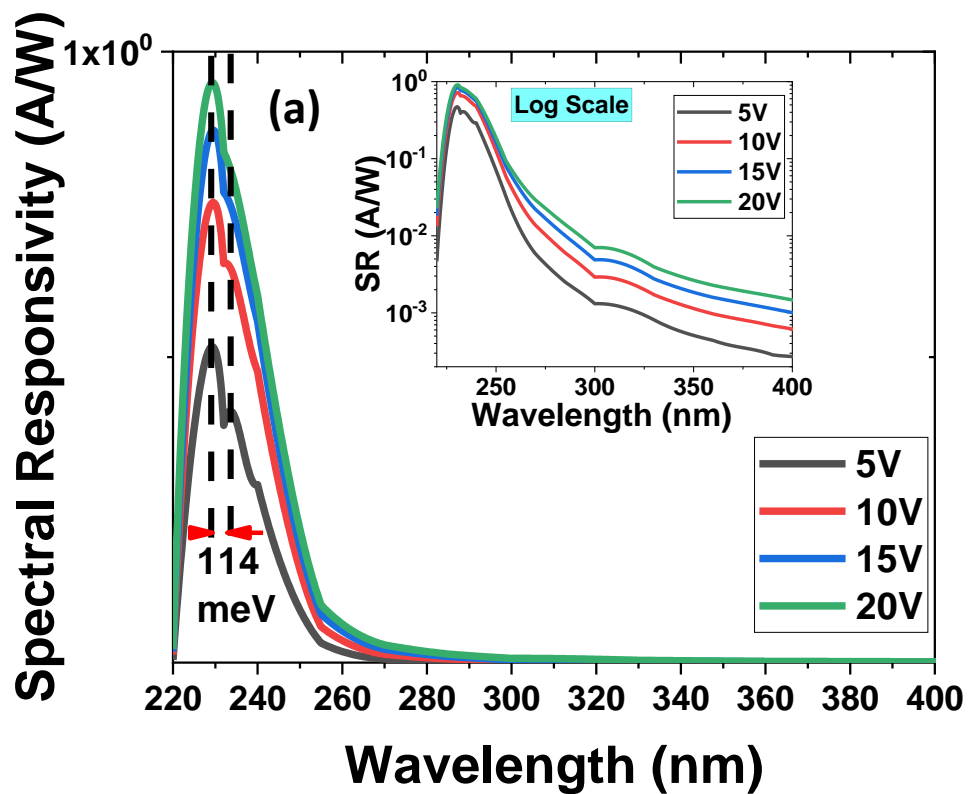


Figure 6 (a). Shows variation of spectral response with wavelength as a function of voltage in linear scale, inset shows variation of SR with wavelength as a function of voltage in log scale. Also can be seen U.V-Visible rejection ratio is $> 10^2$. (b) Variation of photocurrent (at 230 nm) and dark current with applied voltage. (c) Variation of peak SR (at 230 nm) with applied voltage.